INT. J. RADIAT. BIOL. 1989, VOL. 56, NO. 3, 221–237

The irradiation of V79 mammalian cells by protons with energies below 2 MeV.

Part I: Experimental arrangement and measurements of cell survival

M. FOLKARD, K. M. PRISE, B. VOJNOVIC, S. DAVIES, M. J. ROPER and B. D. MICHAEL

Cancer Research Campaign, Gray Laboratory, PO Box 100, Mount Vernon Hospital, Northwood, Middlesex HA6 2JR, U.K.

(Received 6 February 1989; revision received 2 May 1989; accepted 6 May 1989)

The relative biological effectiveness (RBE) has been determined for protons with mean energies of 1·9, 1·15 and 0·76 MeV, from measurements of the survival of V79 Chinese hamster cells. The cells are supported as a monolayer and are swept through a beam of scattered protons produced using a 4 MeV Van de Graaff accelerator. An estimation of the dose and unrestricted linear energy transfer (LET) variation within the sensitive volume of the cells is given for the three proton energies. The RBEs for cell survival (relative to 250 kVp X-rays) at the 10 per cent survival level are 1·6, 1·9 and 3·36 for protons with track-average LETs of 17, 24 and 32 keV μm^{-1} respectively, and the data suggest that protons are most effective at about 40–50 keV μm^{-1}. It is shown that the proton RBEs can be reconciled with those of other light ions if plotted against z^{*2}/β^2 (where z^* is the effective charge and β is the relative velocity) rather than against LET.

1. Introduction

The continued interest in the use of high energy protons for radiotherapy is mainly due to the well-localized dose distribution that can be obtained using this radiation. The radiobiological effects of such beams are reasonably well studied and widely believed to be similar to, or slightly more effective than, therapy X-rays (Urano *et al.* 1980). The characteristics of protons with lower energies (from a few MeV, up to 30–40 MeV) are less well known; studies of the relative biological effectiveness (RBE) and other properties of protons in this energy range have been reported by Boles *et al.* (1969), Bettega *et al.* (1979) and by Perris *et al.* (1986). For protons with energies below 3 MeV, little data exists; recent work by Belli *et al.* (1986, 1987, 1989) shows results for the RBE of protons with energies down to about 0·7 MeV. Measurements of the effectiveness of low-energy protons may increase our understanding of the biophysical mechanisms of radiation action at the microdosimetric level. These measurements are also relevant to the study of the biological action of fast neutrons. A significant fraction of the energy of fast neutrons is transferred to tissue by recoil protons in this energy range. Between 0·1 and 3·0 MeV, the linear energy transfer (LET) of protons varies from about 12 keV μm^{-1} up to a theoretical maximum of about 100 keV/μm in water. It has been shown that helium ions and deuterons are most effective when the LET of the particles is about 100 keV μm^{-1} (Barendsen 1968). There is evidence, however

0020–7616/89 $3.00

(Belli *et al.* 1989), that for protons the maximum effectiveness can be achieved at a much lower LET.

This paper reports the design, construction and dosimetry of an experimental system for irradiating mammalian cells *in vitro* with low energy protons. An analysed, horizontal beam of 4 MeV protons is produced using a Van de Graaff accelerator. The beam is extracted through a thin window to strike a thin gold scattering foil collimated by a narrow vertical slit. Scattered protons are further collimated by a second narrow slit at the entrance to an enclosed chamber. The chamber contains a rotating platter that supports up to 12 samples, each in the form of a cell monolayer on a thin filter. The platter sweeps the samples through the radiation field defined by the two slits. The apparatus is designed so that the temperature and gas environment of the samples can be controlled during the irradiation. Results are presented for the survival of V79 Chinese hamster cells in the dose range 1–10 Gy irradiated by protons with a mean energy of 1·90, 1·15 or 0·75 MeV. These results suggest that the maximum RBE for protons occurs at about 40–50 keV μm^{-1}.

2. Materials and methods

2.1. *Irradiation method*

Protons are produced using the Gray Laboratory 4 MV Van de Graaff accelerator. The accelerated proton beam is analysed twice, defocused and circularly scanned at a frequency of 1 kHz. The scanning and defocusing arrangement is necessary to produce an even dose distribution and to reduce the average power dissipated in the window at typical running conditions (4 MeV, 0·5–2·0 μA). An undesirable feature of using a scanned beam is that the instantaneous dose rate through the window varies roughly sinusoidally at 1 kHz frequency. The beam emerges through a 25 mm diameter by 50 μm thick polyimide (Kapton, Du Pont) window. About 4 mm in front of the window is a 9·6 mg cm^{-2} thick gold scattering foil. The foil is mounted flush against a pair of brass slits that define an effective scattering area of 1 mm wide by 25 mm high.

The sample stage comprises a 37 cm by 37 cm by 6·5 cm sealed aluminium and stainless-steel chamber containing a 29 cm diameter by 2·6 cm thick aluminium and brass platter. The sample stage and its relationship to the scattering foil are depicted in figures 1a and 1b. The platter can rotate around a 1·4 cm diameter stationary stainless-steel hollow axle supported by the chamber. A 22 mm high by 6·4 mm wide by 0·33 mg cm^{-2} mylar window is used to admit protons into the sample chamber. This window is collimated by a second pair of adjustable brass slits arranged so that the edges of the slits are parallel with the radii of the platter. Cells are irradiated as monolayers on the surface of 13 mm diameter filters; up to 12 filters can be loaded onto the platter. During an irradiation the platter rotates so that each sample in turn is swept once through the proton beam defined by the two pairs of slits. The speed of rotation determines the dose to each sample. The inside of the platter is hollow, and by a suitable arrangement of baffles and holes within the axle and the platter, chilled antifreeze can be pumped into one end of the axle, pass through the platter cavity and out of the other end of the axle. This arrangement is very effective in cooling the platter down to near-freezing temperatures, if required. Also, a facility is provided for flushing gas through the sealed chamber volume, although data obtained using this arrangement are not reported here.

The sample stage is mounted in front of the beam on a specially constructed

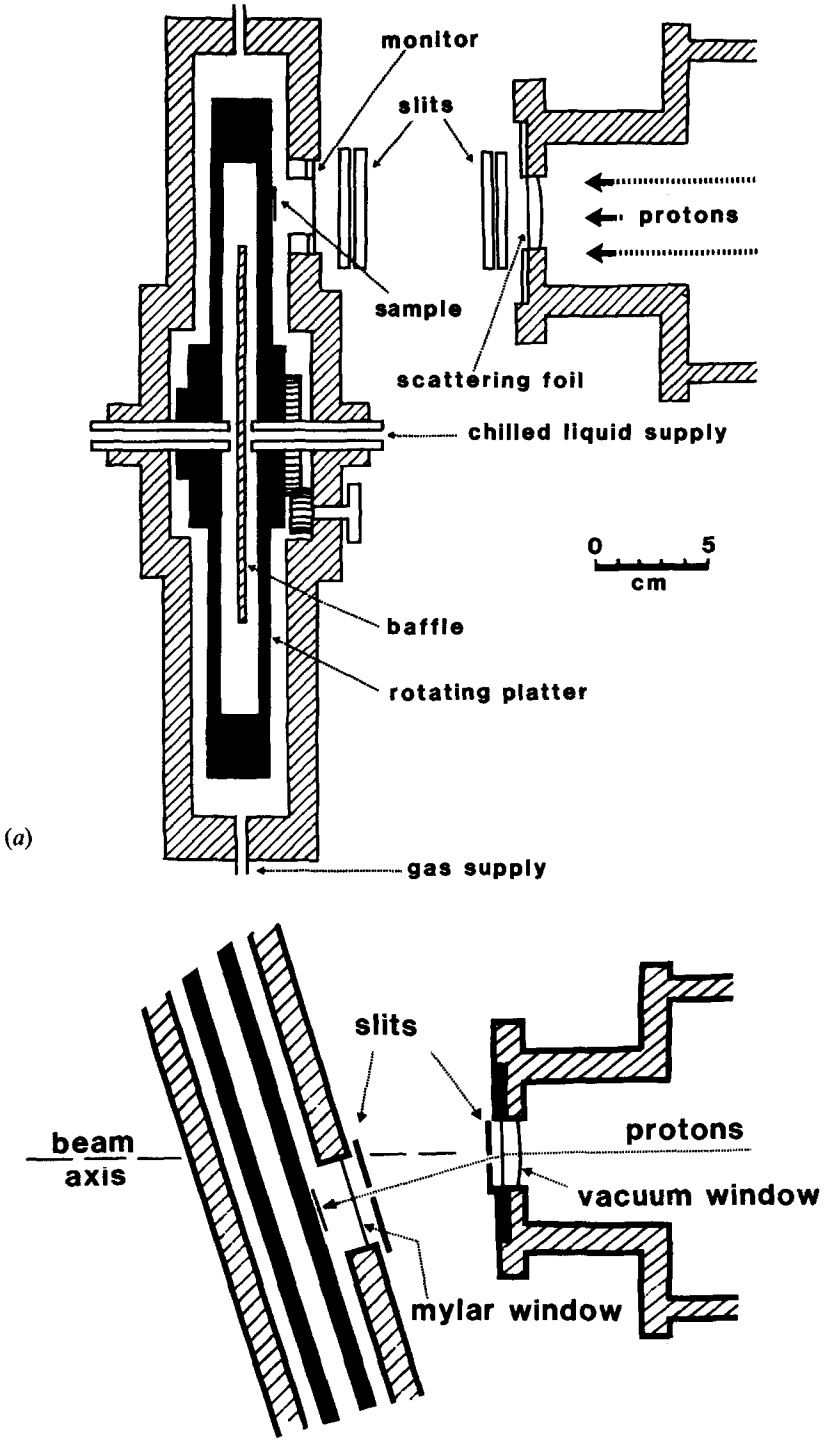

Figure 1. (*a*) Side view of the proton sample stage and source of scattered protons; (*b*) view from above, showing the sample stage offset at an angle of 17° to the Van de Graaff proton beam axis.

platform that allows precise alignment with the scattering foil. The stage is secured to a precision micropositioning table which, in turn, can be positioned on a 11·2 cm wide by 150 mm optical bench (Ealing Electro-optics). The optical bench can pivot at one end, and is arranged so the axis of the pivot is directly below the scattering foil. Therefore both the distance and the angle of the sample stage relative to the scattering foil can be accurately and independently controlled. The flux of scattered protons through the slits decreases rapidly as the off-axis scattering angle is increased. The scattering angle is chosen so that both the flux and the accelerator operating conditions are optimum. Adjustment of the scattering-foil to sample distance is one method used to control the energy of the protons at the sample position, although for some arrangements it is convenient to reduce the proton energy by introducing thin polypropylene (Trespaphan, Hoechst) filters between the foil and the sample. For the experiments described below, three arrangements have been investigated, corresponding to three different incident proton energies (1·90, 1·15 and 0·76 MeV mean energy, see § 3.1) which will be referred to as the high, intermediate and low energy positions. Note that these labels do not necessarily refer to the physical or radiobiological characteristics of the beam; only to their relative energies. The highest energy protons are obtained using a foil–sample distance of 40 mm and a scattering angle of 17·5°. Protons of intermediate energy are obtained by setting the foil–sample distance to 80 mm and the scattering angle to 17°. Finally, the lowest energy protons are obtained at the intermediate energy position by adding a 15 μm thick polypropylene filter between the foil and the sample.

2.2. *Sample preparation*

Chinese hamster V79-379A cells are grown in Eagle's minimal medium modified for suspension cultures and supplemented with 7·5 per cent foetal calf serum. A suspension is concentrated to 1×10^7 ml^{-1} and 20 μl spread as a monolayer onto 13 mm diameter polyvinylidine difluoride membrane filters (Millipore Corporation). The filters are prewashed with cell culture medium and rest on 1 per cent agar set in cell culture medium. The cells remain at 4°C for 15 min for the medium to soak through before they are irradiated. These particular filters are used because they are hydrophilic, and draw virtually all of the surface medium off the cells without the cells drying out. If the medium is not drawn off in this way then the dosimetry calculations would be unreliable. This method of sample preparation has been employed successfully for experiments using 1·5 keV ultrasoft X-rays (Folkard *et al.* 1987) and other poorly penetrating radiations. The ultrasoft X-ray data in particular suggest that no more than 1–2 μm of surface water covers the cell monolayer. The filters also inhibit the cells from attaching so that the cells do not 'flatten-out'. Knowledge of the cell size and shape during the irradiation is necessary for the dosimetry calculations (§ 2.3). This method of sample preparation has been examined using cells stained with 2 mg ml^{-1} Hoechst 33342 in phosphate buffered solution. Inspection using a fluorescence microscope confirms that the cells are spread as a monolayer and that they do not attach to the filter. The membrane filters, with cells to be irradiated, are attached by surface tension onto the cooled sample platter. A moist backing filter (Whatman No. 1) is placed between the membrane filters and the platter to prevent the cells drying out completely. All cell samples are irradiated at 4°C using the cooling arrangement described in § 2.1. The cells are cooled so that they are irradiated using the same

conditions as experiments currently in progress to measure the induction of DNA single- and double-strand breaks by low-energy protons.

After irradiation the cells are washed from the filters, diluted and plated out. After 6 days' incubation at 37°C in an atmosphere of 95 per cent air: 5 per cent CO_2, plates are stained and the colonies containing 50 or more cells are counted.

2.3. *Dosimetry and dose monitoring*

The mylar window through which the protons enter the sample chamber is actually part of a monitor assembly for measuring the dose to the samples during an irradiation. Immediately above and below the window are two 4·8 mm diameter parallel-plate ionization chambers. The polarizing electrode of each chamber is constructed from 0·33 mg cm^{-2} aluminized mylar, and serves as a window for admitting the protons into the chamber cavity. A brass collecting electrode is arranged so the plate spacing is about 1 mm. A polarizing voltage of -350 V is normally used. The current from the two chambers is integrated by converting the current to voltage and then to frequency. The resulting pulses are applied to a six-decade counter so that the number stored in the counter is proportional to the integrated chamber current. The accumulation of pulses also enables an electronic timer that allows the dose rate (counts per second) to be readily calculated. Additionally, an analogue dose-rate meter is used to monitor this quantity during the irradiation.

The monitor assembly is calibrated using an extrapolation-type, parallel plate ionization chamber designed and constructed for use in this experiment. The polarizing electrode is constructed from 0·33 mg cm^{-2} aluminized mylar and the collecting electrode is a 13 mm diameter copper plate surrounded by a 21 mm diameter guard ring. The collecting electrode and guard ring are mounted on one end of a 22 mm diameter precision-threaded cylinder of 1 mm pitch. This engages with the polarizing electrode support and enables the plate spacing to be adjusted accurately down to 0·3 mm with a precision of $\pm 5\,\mu$m and an accuracy of $\pm 20\,\mu$m (ascertained by measurements of the chamber capacitance).

To measure the dose per revolution of the platter, the sample platter is removed and replaced by a rotating-arm assembly which supports the extrapolation chamber. It is arranged so that the centre of the sensitive volume of the chamber is located at a typical sample position. The chamber is then swept through the collimated proton beam at a preset speed and at the same position as the samples and the total electric charge accumulated in one sweep is measured using a Keithley 616 electrometer. This is repeated for several plate spacings to ascertain the limiting charge per unit plate spacing, dQ/dx, for an infinitesimally small collecting volume. For plate spacings less than 1·2 mm, a constant dQ/dx is observed. It was anticipated that sweeping the chamber in this manner would induce spurious electronic charge into the chamber and cables; no such undesirable effect is observed, however, and for a stable proton beam a reproducibility of less than 1 per cent is readily achieved. The dose, D, is calculated using the following expression,

$$D = \frac{W_p}{eA\rho_a} \frac{(\mu/\rho)_s}{(\mu/\rho)_a} k_{tp} k_w \frac{dQ}{dx} \qquad (1)$$

Where e is the electronic charge, A is the effective area of the collecting electrode (136·2 mm^2, determined by capacitance measurements) and ρ_a is the density of air

at STP. W_p is the average energy per ion pair in air for protons. The value used for W_p is 35·2 eV/ion pair, from the measurements of Larson (1958) for 1·8 MeV protons. In the range of proton energies of interest here, W_p is reasonably independent of energy and this value is assumed to apply in all cases. The quantity $(\mu/\rho)_s/(\mu/\rho)_a$ is the ratio of the mass attenuation coefficients of the sample and air. A value of 1·2 is used, based on the stopping power calculations of Barkas and Berger (1964) for 2 MeV protons. The factor k_{tp} is a correction for temperature and pressure, and k_w is a correction for the attentuation of the protons within the cells and within the chamber window. The value of k_w will be discussed in § 3.2.

The monitor chamber is calibrated by relating the number of counts per second from this chamber to the dose received when the sample is swept once through the radiation field at a preset angular velocity. This method of monitoring is reliable only if the dose rate is constant during the irradiation. In practice, the dose rate can be maintained to within 1–2 per cent of the desired value during each sample irradiation. A versatile positioning system has been developed to control the movement of the platter. The position of the samples relative to the irradiation position is determined using a Hall effect device that senses a magnet on the rim of the platter. This positional information enables the signal from the monitor to be gated electronically so that counts are accumulated only when the sample is passing through the radiation field. The speed of the platter (which determines the dose received) is inversely proportional to a number preset using a four-decade thumbwheel switch. Measurements have shown that the change in dose with speed of rotation agrees with the expected change to better than 1 per cent over the range of speeds used (typically, 1 rev min^{-1} to 0·01 rev min^{-1}). The platter stops revolving after each sample has been irradiated, to enable the number of counts per second for that irradiation to be recorded and the appropriate rotation speed for the next irradiation to be entered. Note that the angular velocity must not be too fast, otherwise the irradiation time for *each cell* on the filter will be comparable to the period of the scanned proton beam (1 ms) and an inaccurate dose will be given.

2.4. *Proton beam energy measurements*

The proton energy spectrum for a variety of experimental configurations has been ascertained using a partially depleted (300 μm depletion depth), ruggedized silicon surface-barrier detector (EG & G Ortec, model 017-050-300) with an active area of 50 mm^2. A 3·7 kBq unsealed ^{241}Am isotope source is used to calibrate the detector in vacuum. Conventional spectroscopy electronics are used to process the signal which is fed to a 1024-channel multi-channel analyser (MCA). The detector is located in the proton beam at the sample position by the same arm assembly used to support the extrapolation chamber. A 0·2 mm diameter pinhole is mounted 4 mm in front of the detector to reduce the count rate to a level where dead-time effects in the MCA are not significant.

3. Results and discussion

3.1. *Incident proton energy*

Although the proton beam produced by the Van de Graaff accelerator is almost monoenergetic initially, measurements using the surface-barrier detector show that the protons reaching the sample irradiation position cover a range of energies. The protons have an initial energy of 4 MeV. By measuring the position of the Bragg peak it has been estimated that the protons lose about 750 keV in the polyimide

vacuum window and a further 650 keV in the gold scattering foil. Figure 2 shows the measured energy spectra at the sample position for the low, intermediate and high energy arrangements. The spread in energy may be due to a combination of straggling within the various absorbers and the different paths taken by protons from different points on the scattering foil to reach a point on the sample. No variation in the energy spectrum is observed across the sample region. The shapes of the 'tails' on the low energy side of the energy distributions are strongly influenced by the size of the pinhole used with the surface barrier detector. It is assumed, therefore, that these tails represent scattering from the edges of the pinhole and are subtracted from the data (by assuming the spectra are symmetrical) before the data are used in any calculations. The mean energies for the low, intermediate and high energy positions are 0·76 MeV, 1·15 MeV and 1·90 MeV respectively.

3.2. *Dose and dose distribution measurements*

Below a few MeV, the characteristics of the proton beam can vary significantly within the thickness of a single cell. This is illustrated by figure 3, which depicts the

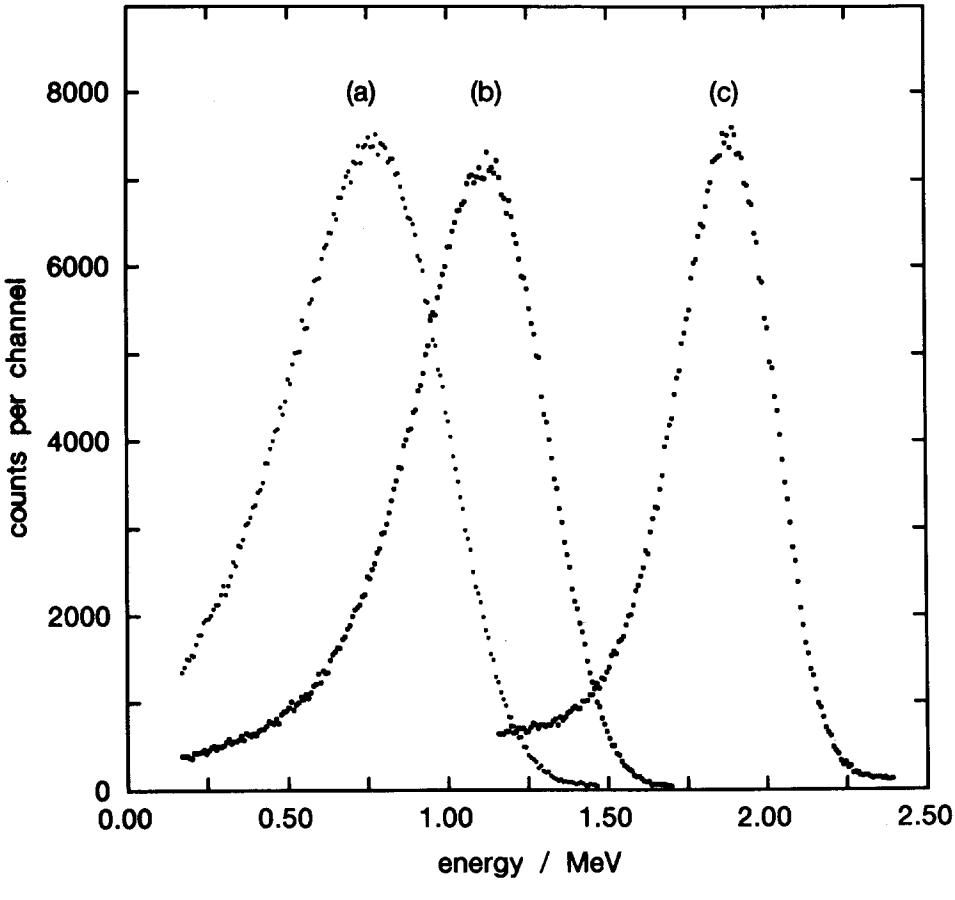

Figure 2. Proton energy spectra at the cell surface for the (**a**) low, (**b**) intermediate and (**c**) high energy positions.

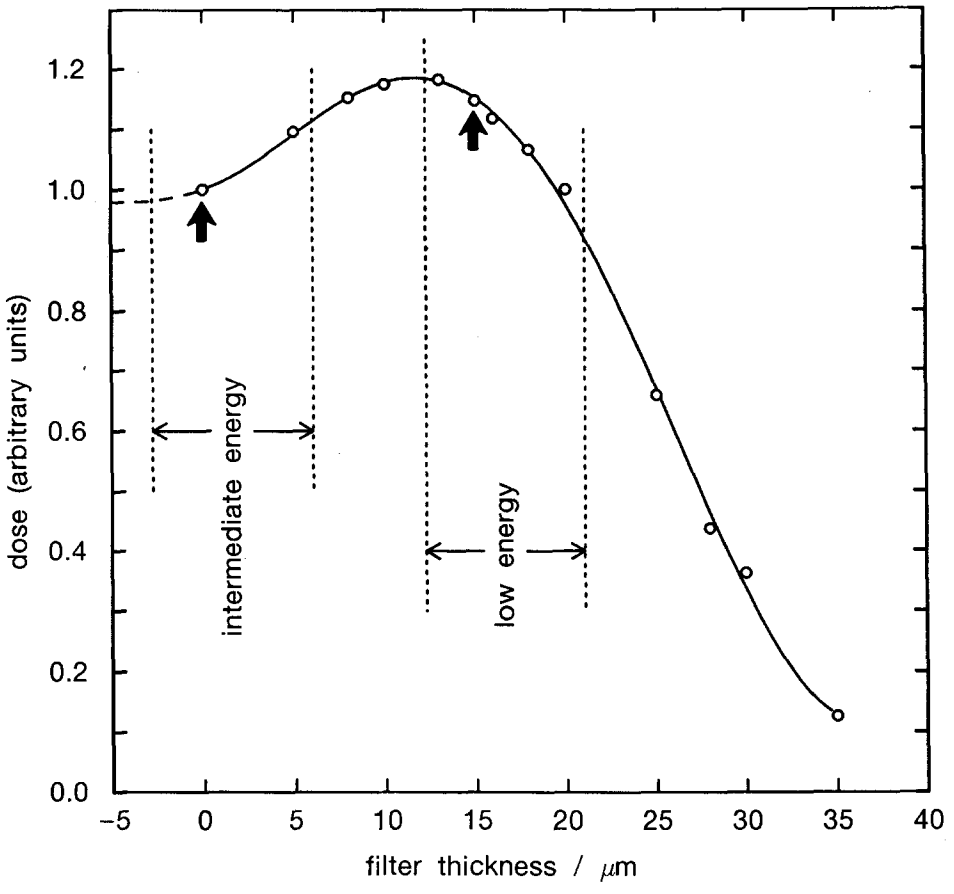

Figure 3. The dose as a function of filter thickness for a scattering angle of 17° and a source–sample distance of 80 mm. The dashed lines indicate the estimated part of the Bragg curve used to irradiate the cell nucleus for the intermediate and low energy arrangements. The arrows represent the dose measured by the extrapolation chamber for these two arrangements.

measured dose as a function of polypropylene filter thickness for the intermediate and low energy position. If the ordinate scale is multiplied by 0·91 (the ratio of the densities of polypropylene and water) then this axis approximately represents cells thickness. The data show the well-known Bragg peak of specific ionization as the proton beam energy is reduced by the absorber. The peak is broadened considerably because of the spread in proton energy. This information can be used to calculate the dose distribution and hence the average dose within the radiation-sensitive site of a *single* cell. To do this it is assumed that our V79 cells are similar to those described in a paper by Datta *et al.* (1976); they depict an unattached cell, 18 μm wide and 10 μm high with a nucleus 15 μm wide and 8 μm high. The measurements made using the fluorescence microscope (§ 2.2) show this to be a reasonable model of our cells. If a correction for density is made (as above) then the data of figure 3 can be used to estimate the region of the depth–dose curve used to irradiate the nucleus of the cell for the intermediate and low energy experiments. These regions are indicated in figure 3; they are offset by $-3{\cdot}8$ μm to allow for the

thickness of the extrapolation chamber window (also corrected for density). Note that for the intermediate energy position the dose *increases* with depth into the cell, and for the low energy position the dose *decreases* with depth. By modelling the cell structure mathematically it is possible to estimate the dose distribution within the cell nucleus. This is depicted in figure 4 for the intermediate and low energy positions relative to the dose measured by the extrapolation chamber. The means of the intermediate and low energy dose distributions are 1·02 and 1·0 respectively (i.e. ≈ 1), therefore no correction is needed for the absorption in the chamber window and within the cell (i.e. in equation 1, $k_w = 1$). Although we have assumed that the whole nucleus constitutes the radiation-sensitive region of the cell, there is evidence that it is only the nuclear membrane that is sensitive (Datta *et al.* 1976, Cole *et al.* 1980). If this assumption is made, then very different dose distributions are obtained; surprisingly, however, the means of both these distributions are still close to 1. For the high energy position, measurements (not shown) reveal that there is little variation of dose with depth; therefore all parts of the cell receive the same dose and, for this position also, $k_w = 1$.

Variability in the dose rate over the sample area (i.e. the filter) will occur if the collimated proton beam is not uniform, or if the edges of the slits are not radial with the rotation axis of the sample platter. Measurements of the dose rate at intervals along the collimated region have been made using a specially constructed thin-window ionization chamber with a 3 mm diameter window. The chamber was swept through the collimated beam at the centre of the sample position and up to ± 6 mm from the centre for all three energy positions. The results are shown in

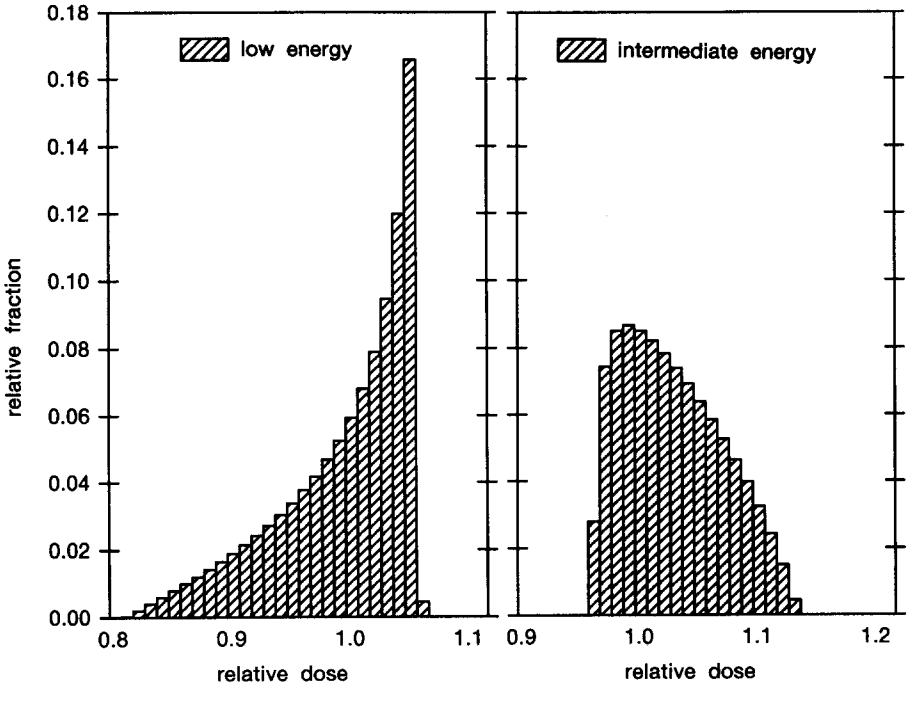

Figure 4. The distribution of dose within a cell nucleus, relative to the dose measured by the extrapolation chamber for the intermediate and low energy positions.

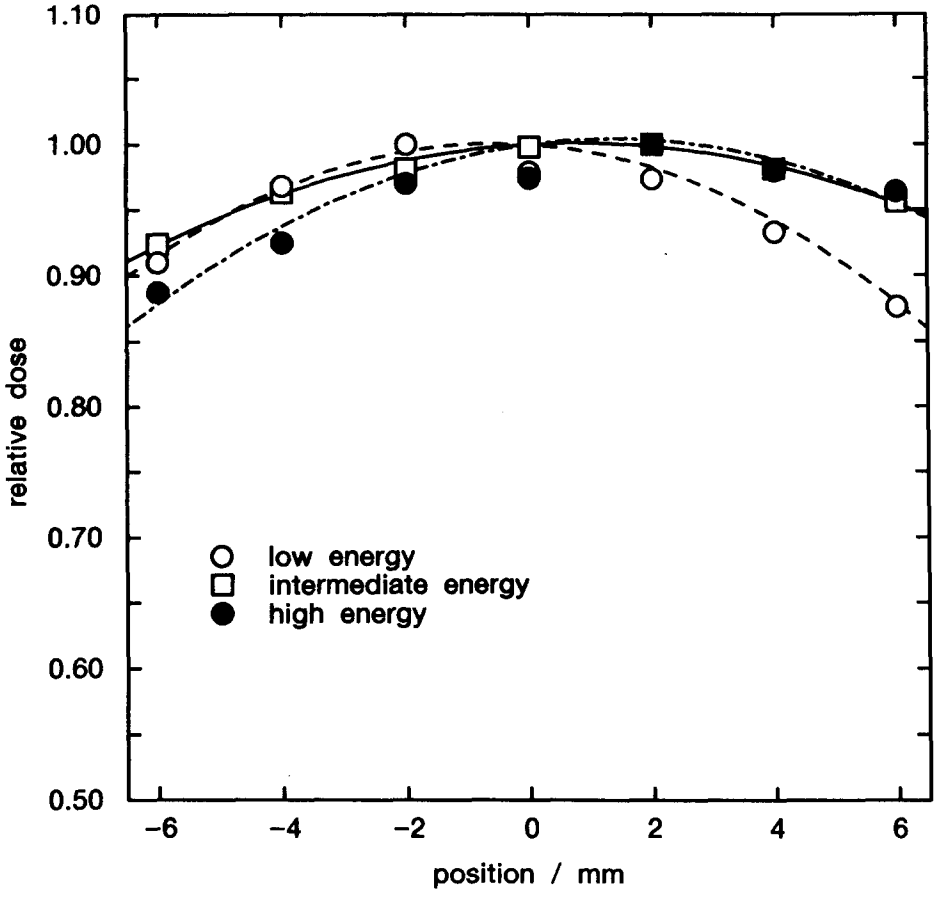

Figure 5. Relative dose variation from the top to the bottom of the filter (relative to the peak dose) for the low, intermediate and high energy positions.

figure 5, and represent the relative dose variation from the top to the bottom of the filter. It is seen that the dose is about 10–12 per cent lower at the upper and lower edges of the filter than at the centre. Because the filter is circular, however, most of the cells will be irradiated by the beam within ± 3–4 mm of the centre of the filter. It can be shown that about 90 per cent of the cells receive a dose which is within ± 3 per cent of the *mean* dose (i.e. the dose measured by the extrapolation chamber).

3.3. *Estimating the LET*

It would be desirable if the range of proton LET values within the cells for a particular arrangement were narrow. This is not the situation, however, for several reasons: firstly because the proton beam at the sample position is not monoenergetic, and secondly because energy is lost as the protons pass through the cell, further spreading the range of energy (and hence LET) within the cell. Even if the protons were monoenergetic throughout the sample, there would still be a spread in LET due to statistical fluctuations in the energy deposited along the track. Using the measurements shown in figure 2, and allowing for the loss of proton energy as the protons pass through the cell (assuming all the cells have the dimensions described

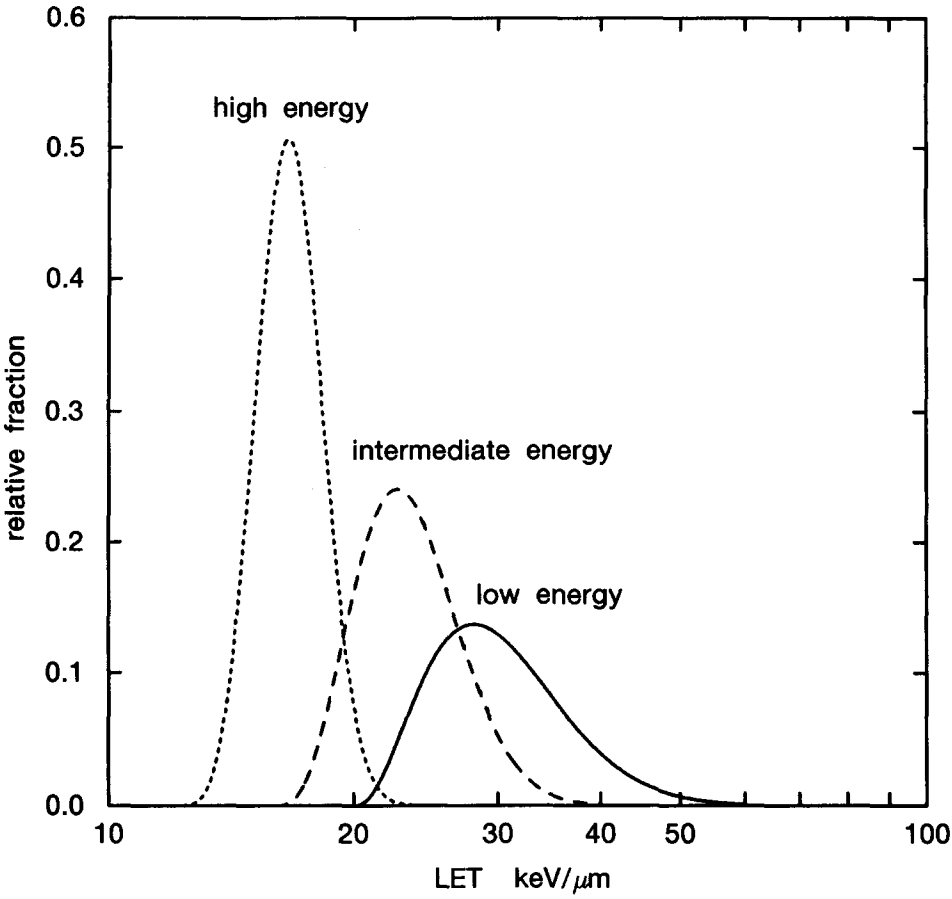

Figure 6. The estimated distribution of LET within the cell nucleus for the low, intermediate and high energy positions.

in § 3.2), it is possible to estimate the unrestricted LET (L_∞) frequency distribution within the nucleus of the cell. This is depicted in figure 6 for the low, intermediate and high energy positions. The calculated low energy proton LET distribution probably underestimates the proportion of high LET events in the spectrum, because it is difficult to estimate precisely the contribution from very low energy protons (below about 200 keV). The track average LET of these distributions are 32, 24, and 17 keV μm^{-1} respectively.

3.4. *Cell survival*

Chinese hamster V79-379A fibroblasts are irradiated in air at the three energy positions described above. The surviving fraction of cells is plotted against dose in figure 7. In all cases a linear quadratic function of the form

$$\text{surviving fraction} = e^{-(\alpha D + \beta D^2)}$$

has been fitted to the logarithm of the data using the method of least-squares. The data are unweighted apart from the two lowest dose points of the high energy survival data. This improves the fit at low doses and has little effect on the

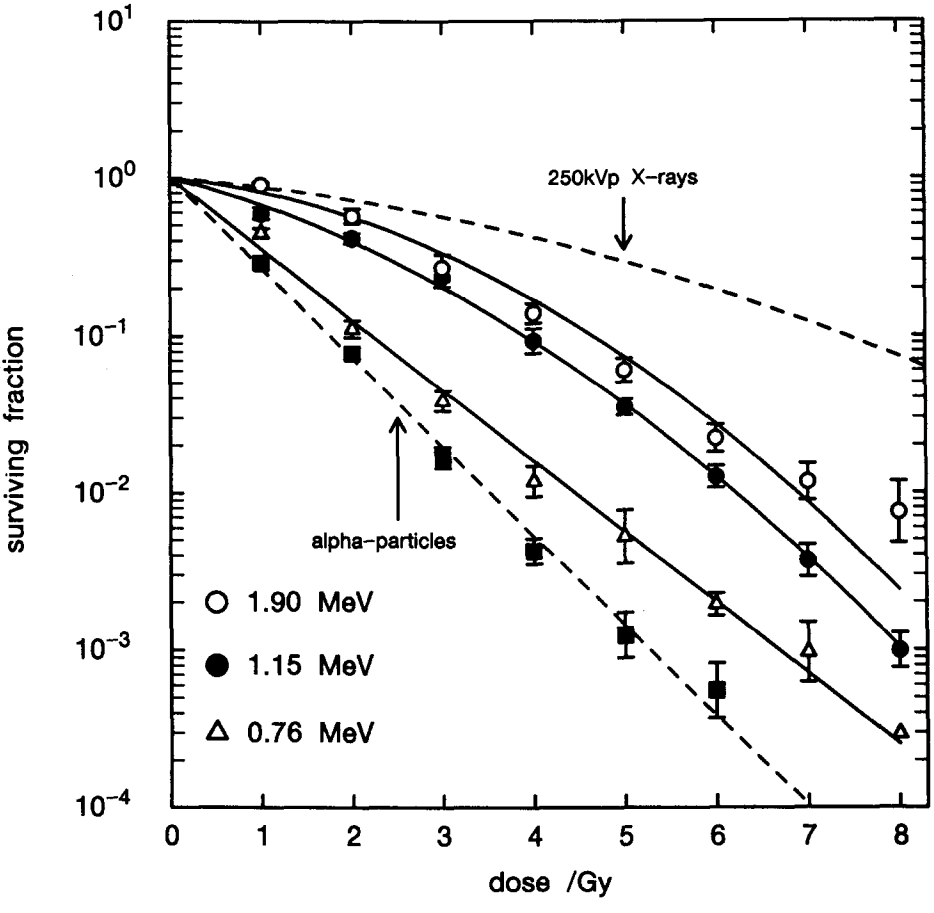

Figure 7. The surviving fraction as a function of dose for V79 Chinese hamster cells irradiated with 1·9 MeV (○), 1·15 MeV (●) and 0·76 MeV (△) protons. Also shown for comparison are the survival curves for V79 cells irradiated with 250 kVp X-rays and 3·8 MeV α-particles.

calculated RBE at 10 per cent survival (see below). The values of the constants, α and β, are summarized in table 1. Each data point is the average surviving fraction for at least five separate experiments, and the error bars are plus or minus one standard error of the mean. Also shown is the cell survival curve obtained for V79 cells in suspension irradiated with 250 kVp X-rays and the data and fitted survival curve for cells irradiated using near-monoenergetic α-particles (FWHM = 500 keV) with a mean energy of 3·8 MeV. The α-particles were produced using a ^{238}Pu source similar to that described by Thacker *et al.* (1982). Cells were prepared for α-particle irradiation using the technique described in § 2.2. The mean LET for the α-particles is approximately 105 keV μm^{-1} and the RBE at the 10 per cent survival level (relative to 250 kVp X-rays) is 4·3. For protons with mean LETs of 17, 24 and 32 keV μm^{-1} the RBEs at the 10 per cent survival level are 1·61, 1·91 and 3·36 respectively. At all survival levels there is clearly an increase in the effectiveness of protons as the mean LET is increased. The data for the 32 keV μm^{-1} protons are reasonably well fitted by a simple exponential, although it is apparent that the data

Table 1. The values of α and β obtained by fitting the linear-quadratic function, surviving fraction $= \exp -(\alpha D + \beta D^2)$ to survival data for cells irradiated with 250 kVp X-rays, α-particles and protons; the RBEs at 10 per cent survival, relative to 250 kVp X-rays, are also given.

	Mean energy	α (Gy^{-1})	β (Gy^{-2})	RBE (10 per cent survival)
X-rays	(250 kVp)	$0{\cdot}11 \pm 0{\cdot}022$	$0{\cdot}027 \pm 0{\cdot}002$	1·00
Protons	1·90 MeV	$0{\cdot}13 \pm 0{\cdot}036$	$0{\cdot}078 \pm 0{\cdot}007$	1·61
Protons	1·15 MeV	$0{\cdot}33 \pm 0{\cdot}038$	$0{\cdot}066 \pm 0{\cdot}005$	1·91
Protons	0·76 MeV	$0{\cdot}03 \pm 0{\cdot}016$	—	3·36
α-Particles	3·89 MeV	$1{\cdot}31 \pm 0{\cdot}023$	—	4·23

exhibit a slight negative curvature. Also, the slope of this curve is less than the final slopes of the two other proton survival curves. These observations may be an indication that some of the cells are not receiving the full estimated dose, perhaps due to partial shielding. Any shielding effects will be critical for these high LET protons because their range in tissue is comparable to the thickness of the cell monolayer. An exponential function fitted only to the low dose points has a slope similar to the final slopes of the other curves, and may be a better estimate of cell survival for the low energy proton irradiations. The RBE at 10 per cent survival for this curve is 3·7 and the α value is $1{\cdot}15\ Gy^{-1}$. Experiments are in progress to see if it possible to measure cell survival at even lower proton energies, using the low energy arrangement described earlier and an extra 5 μm polypropylene filter (so that the total filtration is 20 μm). Preliminary results indicate that the effectiveness is somewhere between low and intermediate energy protons. So far, results have been variable, because a large tail is observed on the data after only 1–10 per cent surviving fraction.

The RBEs for other radiations in this LET range have been investigated previously; Thacker and co-workers (1979) present results for the survival of V79 hamster cells irradiated with helium ions in the range 20–90 keV μm^{-1}, and Barendsen *et al.* (1963) and Barendsen (1964) have studied the survival of T1 human kidney cells irradiated with deuterons and helium ions. The sensitivity of T1 cells is apparently similar to V79 cells (Thacker *et al.* 1979). The RBE data from these two references at the 10 per cent survival level are shown in figure 8, together with the RBEs for protons and the RBE for 110 keV μm^{-1} α-particles. Note that the α-particle RBE point fits the RBE–LET relationship shown. The horizontal lines through the proton data points are the full-width at 10 per cent maximum of the estimated LET distributions (figure 6). The error bars on the RBE values are derived from 'worst-case' fits to the cell survival data (figure 7) after estimating the errors on the dose delivered to the cells. The following errors are assumed: <6 per cent overall uncertainty for W_p and the ratio of the mass attenuation coefficients, $\pm 3{\cdot}5$ per cent uncertainty due to cell size variation and attenuation by surface water (up to 1·5 μm water and 10 per cent variation in size) for the low and intermediate energy experiments (these errors are less for the high energy experiments), ± 3 per cent dose variation due to geometry effects (explained in § 3·2) and ± 1 per cent due to dose-rate fluctuations. It can be seen that the RBEs for the low and medium LET protons are similar to the RBE for helium ions of the same LET. The highest LET

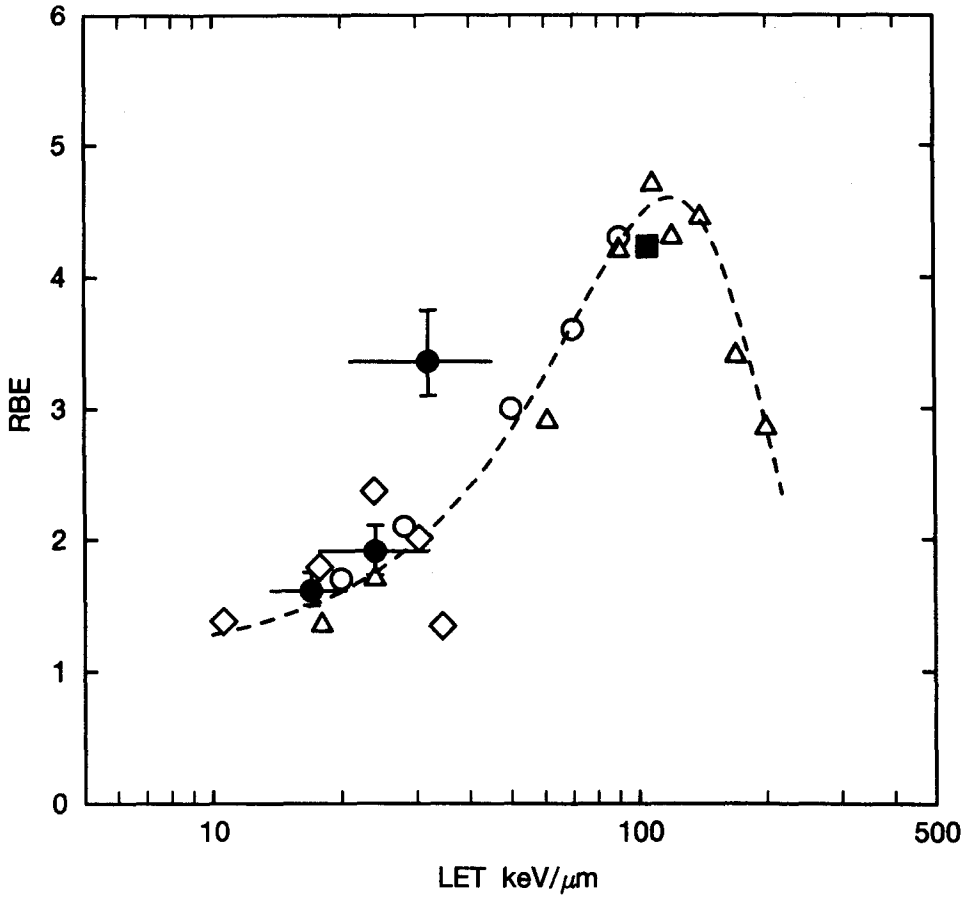

Figure 8. The RBE at the 10 per cent survival level for protons as a function of LET (●). The error bars are explained in the text. The RBE for 3·8 MeV α-particles obtained at this laboratory is included (■). Also shown is the RBE (at 10 per cent survival) for V79 cells irradiated with helium ions (○) (Thacker *et al.* 1979) and the RBE (at 10 per cent survival) for T1 human cells irradiated with deuterons and helium ions (△) (Barendsen et al. 1963, Barendsen 1964). The ◇ symbols are the RBEs at 10 per cent survival of V79 cells irradiated by low energy protons, calculated from recent data by Belli *et al.* 1989.

proton RBE, however, differs significantly from the RBE–LET curve for other light ions. It is apparent from these data that low energy protons with an LET of about 30–40 keV μm^{-1} are significantly more effective than helium ions of comparable LET. If it is assumed that the maximum RBE for protons is about 4–5, then an extrapolation of the data in figure 7 suggests that this maximum occurs for protons with a mean LET of roughly 40 keV μm^{-1}. A comparable result is described in a recent paper by Belli *et al.* (1989). They have irradiated V79 cells attached to mylar foil using protons with energies from 0·73 to 3·36 MeV. The RBEs at the 10 per cent survival level for their data are shown on figure 8. It is apparent that our data are in reasonable agreement with their data up to about 24 keV μm^{-1}. At higher LETs their measured RBEs decrease rapidly with increasing LET, whereas our

data show that 35 keV μm^{-1} protons are significantly more effective than 24 keV μm^{-1} protons. It is possible that this discrepancy is due to the differences in the energy spectra used to irradiate the cells. The distribution of proton energies at the cell surface for our arrangement is significantly greater than for the arrangement used by Belli *et al.* For this reason, and because our cells are thicker (as they are unattached), the spread in LET through the cell nucleus is greater in our system. The presence of protons with LETs down to 20 keV μm^{-1} in the high LET spectrum may be masking the decrease in effectiveness at high LETs observed by Belli *et al.* Another difference is that no shoulder is seen on their survival curve for the 24 keV μm^{-1} proton experiments, and for higher LET protons a strong negative curvature is observed which they attribute to poorly attached or shielded cells not receiving the full dose.

Other investigations of the RBE of low energy protons have been published; Perris *et al.* (1986) have measured the RBE of V79 cells irradiated in plateau phase for protons with LETs of 5·8 keV μm^{-1} and 12·1 keV μm^{-1}. They obtain RBEs of 1·29 and 1·95 at 37 per cent survival respectively (relative to ^{60}Co γ-rays) and show

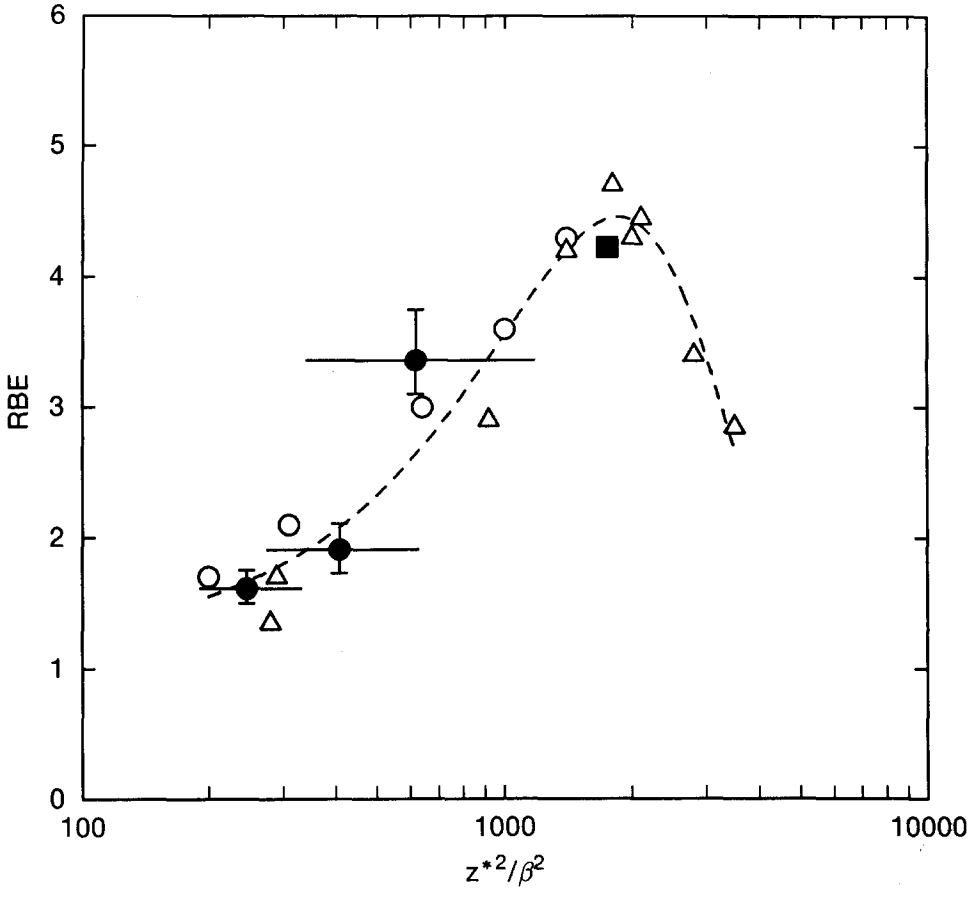

Figure 9. The RBE at the 10 per cent survival level for protons as a function of z^{*2}/β^2 (●). The RBEs for α-particles, helium ions and deuterons are also shown (redrawn from figure 8).

that their results are consistent with data from α-particle irradiations and also with earlier work by Bettega *et al.*, who have measured the RBE of EUE human cells for protons with energies between 8 and 31 MeV. The RBEs at 37 per cent survival for our data are 1·6, 2·1 and 4·6 for 17, 24 and 32 keV μm^{-1} protons, respectively. These points lie on an RBE–LET curve slightly (but not significantly) below a similar curve through the data of Perris *et al.* (1986).

It is well known that LET is not a reliable indicator of the biological effectiveness of ionizing radiations in all cases (ICRU Report 16, 170). For increasingly heavier ions the maximum RBE is shifted to higher values of LET (Kraft and Kraft-Weyrather, 1987). This may be because different ions with the same LET have different particle track structures. A lighter ion has a velocity lower than a heavier ion of the same LET; therefore the secondary electrons produced by the lighter ions are less energetic (and the overall track width is narrower) than those produced by equivalent heavier ions. It has been suggested that the quantity z^{*2}/β^2 may be more appropriate to describe the effectiveness of ions (Katz 1970) where z^* is the effective charge and β is the relative velocity of the ion. This quantity is related to the energy deposited by the secondary electrons. Figure 9 shows the data of figure 8 plotted against z^{*2}/β^2 rather than LET. It is apparent the discrepancies between the RBEs for protons, helium ions and deuterons are less when plotted against this quantity. Thacker *et al.* (1979) show that the effectiveness of accelerated boron and nitrogen ions can also be reconciled in this way.

In conclusion, the data presented here suggest that low energy protons have a high level of effectiveness at an LET lower than for other radiations, and this is a further demonstration that unrestricted LET is of limited use as an indicator of biological effectiveness. Work is in progress to measure how the induction of DNA single-strand and double-strand breaks depends upon the LET and type of irradiating particle, and also to measure the dose-modifying effects of irradiating cells under hypoxia with low energy protons.

References

Barendsen, G. W., 1964, Impairment of the proliferative capacity of human cells in culture by α-particles with different linear-energy transfer. *International Journal of Radiation Biology*, **8**, 453–466.

Barendsen, G. W., 1968, Responses of cultured cells, tumours and normal tissue to radiations of different linear energy transfer. *Current Topics in Radiation Research*, **4**, 293–356.

Barendsen, G. W., Walter, M. D., Fowler, J. F., and Bewley, D. K., 1963, Effects of different ionizing radiations on human cells in tissue culture. III. Experiments with cyclotron-accelerated alpha-particles and deuterons. *Radiation Research*, **18**, 106–119.

Barkas, W. H., and Berger, M. J., 1964, *Tables of Energy Losses and Ranges of Heavy Charged Particles* (NASA SP-3013).

Belli, M., Cherubini, R., Finotto, S., Moshini, G., Sapora, O., Simone, G., and Tabocchini, M. A., 1986, Inactivation of Chinese hamster V79 cells by high LET proton beams. *International Journal of Radiation Biology*, **51**, 931–932.

Belli, M., Cherubini, R., Finotto, S., Moshini, G., Sapora, O., Simone, G. and Tabocchini, M. A., 1987, RBE-LET relationship for inactivation of V79 Chinese hamster cells irradiated by proton beams. *Proceedings of the 8th International Congress of Radiation Research*, edited by E. M. Fielden, J. F. Fowler, J. H. Hendry and D. Scott (London: Taylor and Francis), **1**, 314.

Belli, M., Cherubini, R., Finotto, S., Moshini, G., Sapora, O., Simone, G., and Tabocchini, M. A., 1989, RBE-LET relationship for the survival of V79 cells irradiated with low energy protons. *International Journal of Radiation Biology*, **55**, 93–104.

BETTEGA, D., BIRATTARI, M., BOMBANA, A., FUHRMAN CONTI, A. M., GALLINI, E., PELUCCHI, T., and TALLONE LOMBARDI, T., 1979, Relative biological effectiveness for protons of energies up to 31 MeV. *Radiation Research*, **77**, 85–97.

BOLES, L. A., BLAKE, K. R., PARKER, C. V. JR, and NELSON, J. B., 1969, Physical dosimetry and instrumentation for low-energy proton irradiation of primates. *Radiation Research*, **37**, 261–271.

COLE, A., MEYN, R. E., CHEN, R., CORRY, P. M., and HITTLEMAN, W., 1980, *Radiation Biology in Cancer Research*, edited by R. E. Meyn and H. R. Withers (New York: Raven Press), p. 33.

DATA, R., COLE, A., and ROBINSON, S., 1976, Use of track-end alpha particles from ^{241}Am to study radiosensitive sites in CHO cells. *Radiation Research*, **65**, 139–151.

FOLKARD, M., VOJNOVIC, B., PRISE, K. M., and MICHAEL, B. D., 1987, An arrangement for irradiating cultured mammalian cells with aluminium characteristic ultrasoft X-rays. *Physics in Medicine and Biology*, **31**, 1615–1626.

ICRU REPORT 16, 1970, *Linear Energy Transfer* (Washington, DC: International Commission on Radiation Units and Measurements).

KATZ, R., 1970, RBE, LET and Z^{*2}/β^2 *Health Physics*, **18**, 175.

KRAFT, G., and KRAFT-WEYRATHER, W., 1987, Biophysical aspects of track structure. *Proceedings of the 8th International Congress of Radiation Research*, edited by E. M. Fielden, J. F. Fowler, J. H. Hendry and D. Scott (London: Taylor and Francis), **3**, 29–34.

LARSON, H. V., 1958, Energy loss per ion pair for protons in various gases. *Physics Review*, **112**, 1927–1928.

PERRIS, A., PIALOGLOU, A. A., KATSANOS, A. A., and SIDERIS, E. G., 1986, Biological effectiveness of low energy protons. I. Survival of Chinese hamster cells. *International Journal of Radiation Biology*, **50**, 1093–1101.

THACKER, J., STRETCH, A., and STEPHENS, M. A., 1979, Mutation and inactivation of cultured mammalian cells exposed to beams of accelerated heavy ions. II. Chinese hamster V79 cells. *International Journal of Radiation Biology*, **36**, 137–148.

THACKER, J., STRETCH, A., and GOODHEAD, D. T., 1982, The mutagencity of α-particles from plutonium-238. *Radiation Research*, **92**, 343–352.

URANO, M., GOITEIN, M., VERHEY, L., MENDIONDO, O., SUIT, H. D., and KOEHLER, H. D., 1980, Relative biological effectiveness of a high energy modulated proton beam using spontaneous murine tumor *in vivo*. *International Journal of Radiation, Oncology, Biology and Physics*, **6**, 1187–1193.